Int. J. Multiphase Flow Vol. 14, No. 4, pp. 483–506, 1988
Printed in Great Britain

0301-9322/88 $3.00 + 0.00
Pergamon Press/Elsevier

LOW REYNOLDS NUMBER MOTION OF A DROPLET BETWEEN TWO PARALLEL PLATES

M. SHAPIRA and S. HABER
Department of Mechanical Engineering, Technion, Israel Institute of Technology, Haifa, Israel

(*Received* 6 *January* 1987; *in revised form* 2 *March* 1988)

Abstract—The low Reynolds number hydrodynamics of a droplet moving in a quiescent fluid between two parallel flat plates is studied. The method of reflections is utilized to obtain approximate solutions for the pressure field, the drag force exerted on the droplet and the deformation of the droplet.

Key Words: creeping flow, bubbles, droplets, wall effects

1. INTRODUCTION

The low Reynolds number motion of small droplets moving in a narrow gap occupied by liquid is of considerable practical interest. The effect of small spherical rigid particles, droplets or bubbles on the performance of hydrodynamic bearings is just one case out of many dealt with in the literature. It was theoretically investigated by Haber *et al.* (1987) who addressed two particular cases: the effect of particles suspended in the lubricating film of a long Rayleigh slider and their effect on a long journal bearing. For both cases it was shown that the load carrying capacity is negligibly affected by the presence of the particles (rigid spheres or droplets), whereas the friction is increased appreciably. Utilizing the low Reynolds number solution for a *single* droplet interacting with two walls, but not with adjacent droplets, they obtained the integrated effect of a dilute suspension on the bearing performance. Thus, the basic flow problem is a superposition of: (a) the flow field around a single droplet moving in a narrow gap occupied by a quiescent liquid; (b) the flow field around a single droplet at rest submerged in Couette flow; and (c) the flow field around a droplet at rest submerged in two-dimensional Poiseuille flow.

In this paper only problem (a) is addressed; the other two will be the subject of a subsequent paper.

Problems concerning rigid particles moving slowly in viscous flows have extensively been treated in the past. Problems concerning droplets caught less attention and are of a higher degree of difficulty due to the fact that the shape of the droplet is *a priori* unknown and that an additional flow field internal to the droplet must be solved.

Generally, any solution that is obtained for droplets can be applied to bubbles or rigid particles since they can be viewed as droplets of zero or infinite viscosity, respectively.

The flow field around a droplet moving in an unbounded fluid can be viewed as a zero-order approximation of a bounded case if the ratio between the diameter of the droplet and its distance from the walls is much smaller than unity.

The flow field around a rigid sphere moving in an arbitrary unbounded flow was presented by Happel & Brenner (1973). Hetsroni & Haber (1970) generalized this solution by treating droplets. In addition, they presented a first-order approximation for the distortion of the droplet shape, assuming that the ratio between shear and surface tension forces is small. Haber & Hetsroni (1971) further extended their solution to obtain a second-order approximation for the flow around a droplet moving in an arbitrary unbounded flow field. For the case of Poiseuille flow they showed that the droplet would translate perpendicular to the cylinder axis.

Youngren & Acrivos (1976) developed a numerical technique to calculate the steady deformation of an inviscid droplet placed in an extensional flow. The three-dimensional Stokes equations for the flow outside the droplet were replaced by a two-dimensional integral equation to be satisfied on the surface of the droplet. The droplet shape was adjusted until the zero normal velocity

condition was satisfied. Rallison & Acrivos (1978) extended their method to include the case of viscous droplets. Special attention was paid to the case of uniaxial extensional flow for which the time-dependent distortion of an initially spherical droplet was calculated.

Three major approaches were used in the past to solve the low Reynolds number flow in particulate systems: the exact analytical approach utilizing curvilinear coordinates; the approximate method of reflections; and the numerical method of collocation.

Stimson & Jeffery (1926) used the bipolar coordinate system to solve the case of two rigid spheres of equal diameter moving along their line of centers. Brenner (1961) used the same coordinates to obtain the flow fields around a rigid sphere which translates towards a flat rigid wall and towards a flat free surface. Dean & O'Neill (1963) and O'Neill (1964) used the bipolar coordinates to obtain the three-dimensional solution for a revolving rigid sphere near one wall. Goldman *et al.* (1967a, b) extrapolated the results obtained by Stimson & Jeffery (1926) to include zero gap thickness. Haber *et al.* (1974) utilized the same coordinates to obtain the general solution for two spherical droplets of various sizes translating along their line of centers in a stationary fluid. As particular cases, one can derive the case of two rigid spheres moving along their line of centers (the liquid viscosities inside the droplets are set to infinity), the case of a droplet moving towards a rigid surface (the radius of one droplet and the liquid viscosity inside it are set to infinity) and the case of a droplet moving towards a free surface (the radius of one droplet is set to infinity and the viscosity of the liquid inside it is set to zero). For the case where a particle touches the wall, O'Neill (1968) and Goren (1970) used the tangent sphere coordinate system to enhance convergence of the solution series.

For all the above cases an analytical solution was obtained since it was possible to describe the boundaries by fixing a single coordinate in a particular coordinate system. When the boundaries consist of two walls and a sphere no such coordinate system is known to exist. However, the previously mentioned cases form asymptotic solutions for the case of a droplet placed at a large distance from one wall and at close vicinity to the other.

A solution method that accounts for topologically different boundaries was described by Happel & Brenner (1973) and is known as the method of reflections. There is no proof of its uniform convergence, however, in particular systems it can be shown that the contribution of the nth reflection is of the order of $(a/h)^n$, where a is the particle radius and h is the distance of the droplet from the nearest wall. The solution converges very rapidly for ratios of $a/h < 0.2$, quite poorly for $a/h > 0.8$ and blows up for $a/h = 1$. In our case, where the boundaries consist of two flat walls and a sphere, Lamb's (1932) solution in spherical coordinates was used to find the odd reflections which satisfy the boundary conditions over the sphere's surface. A general solution for Stokes equations in cartesian coordinates provided for the even reflections which satisfy the boundary conditions over the walls.

The flow field around a rigid sphere moving between two parallel plates was analyzed by Happel & Brenner (1973). Numerical values were obtained for the drag force exerted on the sphere for only two specific lateral locations of the sphere ($h/H = 0.25, 0.50$).

It is shown in Happel & Benner (1973) how to utilize the same method to obtain the solution for the flow field around a stationary rigid sphere in Couette and plane Poiseuille flow. The method of reflections was also used to obtain the drag force exerted on a rigid sphere moving perpendicular to a wall. Comparison of this solution with the exact solution given by Brenner (1961) shows that an approximate solution composed of two reflections only is in very good agreement with the exact solution when $a/h < 0.1$.

Wakiya (1953) also used the method of reflections to obtain the solution for a rigid sphere moving in a circular pipe. Here, a general solution for Stokes equations in cylindrical coordinates was employed to satisfy the boundary conditions over the pipe's walls. Hetsroni *et al.* (1970) used the same method to solve the problem for a droplet moving in Poiseuille flow.

Ho & Leal (1974) analyzed weak inertia effects for a rigid sphere moving in Couette and plane Poiseuille flow utilizing a regular perturbation scheme. As a zero-order solution they used Faxen's derivation.

Sano & Hasimoto (1978) developed a reflection method by which the flow field around a sphere moving between nonparallel walls was derived.

Up until now and to the best of our knowledge, there is no other analytical method by which these difficult problems can be solved.

Gluckman *et al.* (1971) were the first to develop the semi-analytical collocation method for unbounded multiparticle axisymmetric Stokes flows. Ganatos *et al.* (1978) investigated the case of two and three rigid spheres translating in an unbounded asymmetric field using the collocation method. The main problem that they enountered was how to pick the collocation points so that the scheme yields correct results. Comparison with the exact solution of Stimson & Jeffery (1926) showed that 12 properly located collocation points were sufficient to yield a very good agreement.

Ganatos *et al.* (1980a, b) solved for a rigid sphere moving in a general direction between two parallel walls. Dagan *et al.* (1982) used the collocation method to obtain the solution for a rigid sphere translating near a finite wall.

Normally, the collocation method is not limited to cases where $a/h \ll 1$. Comparison between the collocation method and the method of reflections shows that the numerical results coincide for $a/h < 0.2$.

Experiments with a single particle or droplet or multiparticle systems have been conducted extensively in the past.

Taylor (1934) carried out experiments with a droplet in Couette and hyperbolic flows. He found that the droplets deform and possess an ellipsoidal shape when the ratio between the shear forces and the surface tension is <0.2. This observation validates the assumption that for small distortion parameters the droplet is nearly spherical and as a zero-order approximation a spherical shape can be assumed.

Goldman & Mason (1962) investigated the motion of a droplet in Poiseuille flow. They observed that the droplets perform a slow radial translation within the tube and that it increases with the distortion parameter. The experiments confirmed qualitatively the solutions obtained by Taylor (1932).

Tachibana (1973) let a rigid sphere translate in a pipe due to gravitational forces and reported that for $\mathrm{Re} = 5$ to 8 the rigid spheres translate almost parallel to the walls. These results confirm the theoretical work by Ho & Leal (1974).

Ho & Leal (1975) let a droplet translate in a circular pipe under gravity. Their results show that the droplet deviation from sphericity increases with the distortion parameter. This observation confirms the results obtained by Hetsroni *et al.* (1970). An experiment similar to Tachibana's (1973) was conducted by Miyamura *et al.* (1980) for a rigid sphere translating between two parallel infinite walls and in conduits of square and triangular cross sections. These experiments confirm Faxen's work for $a/h < 0.2$.

Coutanceau & Thizon (1981) examined a bubble translating in a pipe. They found that for low Reynolds numbers and $a/h < 0.2$, the bubble remains almost spherical For $a/h > 0.6$ it has a cylindrical shape enclosed with two spherical caps. In the intermediate range it has an ellipsiodal shape.

The above experiments prove that, for the case of a droplet moving between two parallel walls, the method of curvilinear coordinates is not feasible. The method of collocation can not be used either, since, the location of the surface of the droplet is not *a priori* known. Thus, the method of reflections seems to have the main attraction, although we are limited to large separations between the droplet and the walls.

The mathematical solution for the flow fields is based on the methods introduced by Liron & Mochon (1976). The derivation of the drag force and of the deformation of the droplet is based on the analysis given in Hetsroni & Haber (1970) for a droplet submerged in an unbounded arbitrary flow field and a given small distortion parameter.

2. STATEMENT OF THE PROBLEM

Consider a droplet moving in a quiescent fluid between two parallel flat plates at an arbitrary lateral location. The droplet translates parallel to the plates and maintains a constant velocity U_0.

The distance, H, between the two plates and the distance, h, of the center of the droplet from the lower plate are fixed. In the stationary cartesian coordinate system chosen, the plates are defined by $z = 0$ and $z = H$, and the droplet velocity is given by $U_0\mathbf{i}$, where $\mathbf{i}$ is a unit vector in the x direction (see figure 1).

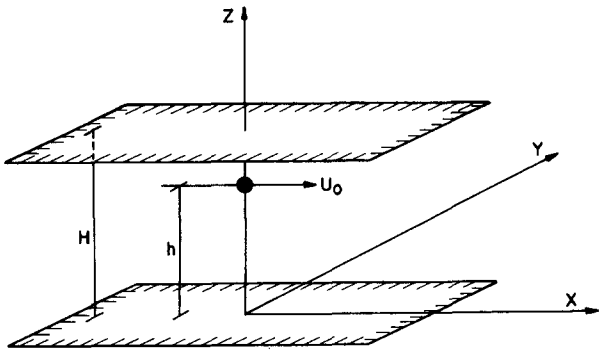

Figure 1. Configuration of the problem.

The fluids involved are assumed to be homogeneous, isothermal, Newtonian and of constant densities. The flow around the droplet is creeping, in other words, inertia terms in the momentum equations are negligible.

With these assumptions the momentum and the continuity equations are as follows:

for the continuous fluid,

$$\nabla^2\mathbf{u} = \frac{1}{\mu}\nabla p$$
$$\nabla\cdot\mathbf{u} = 0; \qquad [1]$$

for the fluid in the interior of the droplet,

$$\nabla^2\mathbf{u}' = \frac{1}{\mu'}\nabla p'$$
$$\nabla\cdot\mathbf{u}' = 0; \qquad [2]$$

where $\mathbf{u}$ and $\mathbf{u}'$ are the velocities exterior and interior to the droplet respectively, p and p' are the pressures and μ and μ' are the respective viscosities.

The boundary conditions are as follows:

at $z = 0$ and $z = H$ (on the plates),

$$\mathbf{u} = 0; \qquad [3]$$

at the surface of the droplet,

$$\mathbf{u}' = \mathbf{u}, \qquad [4]$$

$$\tau_n - \tau_n' = \sigma\left(\frac{1}{R_1} + \frac{1}{R_2}\right)\mathbf{i}_n, \qquad [5]$$

$$\mathbf{u}\cdot\mathbf{i}_n = U_0\mathbf{i}\cdot\mathbf{i}_n; \qquad [6]$$

where $\mathbf{i}_n$ is a unit vector normal to the interface, τ_n and τ_n' are the normal stress vectors ($\tau_n = \tau\cdot\mathbf{i}_n$) based on the velocities $\mathbf{u}$ and $\mathbf{u}'$ respectively, R_1 and R_2 are the principal radii and σ is the surface tension.

3. THE SOLUTION

The solution of the field equations with the given boundary conditions, should explicitly yield the flow field in the interior of the droplet and exterior to it, as well as the general equation of

the interface. However, the simultaneous solution of the flow fields and of the interface equation is a formidable task. An iterative procedure is therefore adopted. For a start, the droplet is postulated to be spherical, and the flow fields are determined independent of the normal component of boundary condition [5]. Later, this latter condition is utilized to determine the deviation of the interface from sphericity; and the interface thus determined can then be used for a second iteration of the flow fields.

From experimental observation it is well-known that small droplets and bubbles migrating under gravity are nearly spherical. Therefore, the calculations start out by assuming the droplet to be spherical.

The solution is based on the method of reflection described by Happel & Brenner (1973). It consists of a sum of velocity fields, all of which satisfy [1] for the velocity field of the continuous medium and [2] for the velocity field interior to the droplet. Each of the solutions partially satisfies the boundary conditions.

The reflected fields are

$$\mathbf{u} = \sum_{K=1}^{\infty} \mathbf{u}_K \qquad [7a]$$

and

$$\mathbf{u}' = \sum_{K=1}^{\infty} \mathbf{u}'_{2K-1}, \qquad [7b]$$

where the summation subscript indicates the reflection number.

The boundary conditions to be satisfied by the reflected fields are as follows:

for the first reflection,

$$\mathbf{u}_1 = 0 \quad \text{at} \quad r \to \infty \qquad [8]$$

and at $r = a$

$$\mathbf{u}_1 = \mathbf{u}'_1, \qquad [9a]$$

$$\mathbf{u}_1 \cdot \mathbf{i}_r = U_0 \mathbf{i} \cdot \mathbf{i}_r, \qquad [9b]$$

$$(\mathbf{I} - \mathbf{i}_r \mathbf{i}_r) \cdot (\boldsymbol{\tau}_{r_1} - \boldsymbol{\tau}'_{r_1}) = 0; \qquad [9c]$$

for the $2K$th reflection ($K = 1, 2 \ldots$) at $z = 0$, $z = H$,

$$\mathbf{u}_{2K} + \mathbf{u}_{2K-1} = 0; \qquad [10]$$

for the $(2K + 1)$th reflection ($K = 1, 2 \ldots$) at $r \to \infty$,

$$\mathbf{u}_{2K+1} = 0 \qquad [11]$$

and at $r = a$

$$\mathbf{u}_{2K+1} + \mathbf{u}_{2K} = \mathbf{u}'_{2K+1}, \qquad [12a]$$

$$\mathbf{u}'_{2K+1} \cdot \mathbf{i}_r = 0, \qquad [12b]$$

$$(\mathbf{I} - \mathbf{i}_r \mathbf{i}_r)(\boldsymbol{\tau}_{r_{2K+1}} + \boldsymbol{\tau}_{r_{2K}} - \boldsymbol{\tau}'_{r_{2K+1}}) = 0; \qquad [12c]$$

where r denotes the radial coordinate and a is the radius of the droplet.

By direct substitution it can easily be verified that $\mathbf{u}$ and $\mathbf{u}'$ as defined in [7a, b] satisfy boundary conditions [3]–[6].

3.1. The First Reflection

The first reflection is the solution for the flow in and around a droplet moving in an unbounded quiescent field. It yielded the following expressions for the velocity components and the pressure outside the droplet:

$$\mathbf{u}_1 \cdot \mathbf{i} = B_1\left[\frac{U_0 a}{2}\left(\frac{1}{r}+\frac{x^2}{r^3}\right)\right] + B_2\left[U_0 a^3\left(\frac{1}{r^3}-3\frac{x^2}{r^5}\right)\right]$$

$$\mathbf{u}_1 \cdot \mathbf{j} = B_1\left[\frac{U_0 a}{2}\frac{xy}{r^3}\right] + B_2\left[U_0 a^3 \frac{-3xy}{r^5}\right] \qquad [13]$$

and

$$\mathbf{u}_1 \cdot \mathbf{k} = B_1\left[\frac{U_0 a}{2}\frac{xz}{r^3}\right] + B_2\left[U_0 a^3 \frac{-3xz}{r^5}\right]$$

$$p = B_1\left[\mu U_0 a \frac{x}{r^3}\right]. \qquad [14]$$

Here the origin of the coordinate system is located at the center of the droplet, and $\mathbf{i}$, $\mathbf{j}$ and $\mathbf{k}$ denote unit vectors in the x, y and z directions, respectively. The coefficients, B_1 and B_2, are functions of the viscosity ratio $\lambda = \mu'/\mu$, namely

$$B_1 = \frac{1+\frac{2}{3}\lambda}{1+\lambda}$$

$$B_2 = \frac{\frac{\lambda}{4}}{1+\lambda}. \qquad [15]$$

3.2. The Second Reflection

The only boundary conditions to be satisfied by the second reflection are

$$\mathbf{u}_1 + \mathbf{u}_2 = \mathbf{0} \quad \text{at} \quad z = 0, z = H. \qquad [16]$$

The solution for $\mathbf{u}_2$ is constructed in two steps. For the first step image droplets are so distributed as to make two components of $\mathbf{u}_1 + \mathbf{u}_2$ vanish on both boundaries. For the second step we solve for a correction field, using a two-dimensional Fourier transform, so that the third component vanishes on the boundaries.

Thus, the solution for $\mathbf{u}_2$ has the following form:

$$\mathbf{u}_2 = \mathbf{v}' + \mathbf{w}, \qquad [17]$$

where $\mathbf{v}'$ stands for the flow field induced by the image droplets, and $\mathbf{w}$ denotes the correction field. A better view of the symmetry of the solution is obtained if a field $\mathbf{v}$ is defined by

$$\mathbf{v} = \mathbf{u}_1 + \mathbf{v}',$$

where $\mathbf{v}$ is the velocity field induced by the droplet *together* with all its image reflections. Hence, w must negate the value of $\mathbf{v}$ on the plates to satisfy [16].

3.2.1. The first step (reflect image drops)

The sum $\mathbf{v}$ of the flow field induced by the droplet and its images (see figure 2) is symmetrical

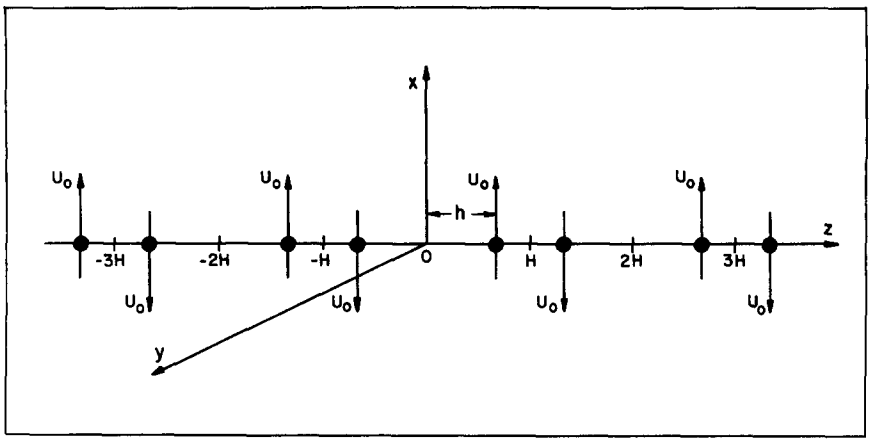

Figure 2. The droplet and its reflected images.

around $z = 0$ and $z = H$. This ensures that the components of the velocity $\mathbf{v}$ parallel to the boundaries vanish.

The cartesian components of $\mathbf{v}$ are†

$$\left.\begin{aligned}
\mathbf{v}\cdot\mathbf{i} &= B_1\frac{U_0 a}{2}\sum_{n=-\infty}^{\infty}\left[\left(\frac{1}{r_n}-\frac{1}{R_n}\right)+\left(\frac{x^2}{r_n^3}-\frac{x^2}{R_n^3}\right)\right] \\
&\quad + B_2 U_0 a^3\sum_{n=-\infty}^{\infty}\left[\left(\frac{1}{r_n^3}-\frac{1}{R_n^3}\right)+\left(\frac{-3x^2}{r_n^5}-\frac{-3x^2}{R_n^5}\right)\right] \\
\mathbf{v}\cdot\mathbf{j} &= B_1\frac{U_0 a}{2}\sum_{n=-\infty}^{\infty}\left(\frac{xy}{r_n^3}-\frac{xy}{R_n^3}\right)+B_2 U_0 a^3\sum_{n=-\infty}^{\infty}\left(\frac{-3xy}{r_n^5}-\frac{-3xy}{R_n^5}\right) \\
\mathbf{v}\cdot\mathbf{k} &= B_1\frac{U_0 a}{2}\sum_{n=-\infty}^{\infty}\left[\frac{x(z-h+2nH)}{r_n^3}-\frac{x(z+h+2nH)}{R_n^3}\right] \\
&\quad + B_2 U_0 a^3\sum_{n=-\infty}^{\infty}\left[\frac{-3x(z-h+2nH)}{r_n^5}-\frac{-3x(z+h+2nH)}{R_n^5}\right]
\end{aligned}\right\} \quad [18]$$

and the associated pressure field induced by the image reflections is

$$q = B_1\mu U_0 a\sum_{n=-\infty}^{\infty}\left(\frac{x}{r_n^3}-\frac{x}{R_n^3}\right), \quad [19]$$

where

$$r_n^2 = \rho^2 + (z-h+2nH)^2, \quad [20a]$$

$$R_n^2 = \rho^2 + (z+h+2nH)^2 \quad [20b]$$

and

$$\rho^2 = x^2 + y^2. \quad [21]$$

†The terms preceded by B_2 would eventually be neglected since their contribution is of the order of $(a/h)^3$, whereas the order of accuracy in this paper is $(a/h)^2$. However, they were not discarded, in case higher-order approximations are attempted by others in the future.

By using the Lipshitz integral as shown by Liron & Mochon (1976) the following results are obtained (see the detailed derivation in appendix A):

for $0 < z < h$,

$$\sum_{n=-\infty}^{\infty}\left(\frac{1}{r_n}-\frac{1}{R_n}\right)=2\int_0^{\infty}J_0(\rho\xi)\frac{\sinh[\xi(H-h)]}{\sinh(\xi H)}\sinh(\xi z)\,\mathrm{d}\xi; \tag{22a}$$

and for $h < z < H$,

$$\sum_{n=-\infty}^{\infty}\left(\frac{1}{r_n}-\frac{1}{R_n}\right)=2\int_0^{\infty}J_0(\rho\xi)\frac{\sinh(\xi h)}{\sinh(\xi H)}\sinh[\xi(H-z)]\,\mathrm{d}\xi. \tag{22b}$$

Identities [22a, b] and their derivatives make it possible to transform equations [18] and [19] into an integral form, in a manner similar to Liron & Mochon (1976), namely:

for $0 < z < h$,

$$\left.\begin{aligned}
\mathbf{v}\cdot\mathbf{i} &= B_1U_0a\int_0^{\infty}\left[J_0(\rho\xi)+\frac{x^2\xi}{\rho}J_1(\xi\rho)\right]\frac{\sinh[\xi(H-h)]}{\sinh(\xi H)}\sinh(\xi z)\,\mathrm{d}\xi\\
&\quad+B_2U_0a^3\int_0^{\infty}2\left[\left(\frac{1}{\rho}-2\frac{x^2}{\rho^3}\right)\xi J_1(\xi\rho)+\left(\frac{x}{\rho}\right)^2\xi^2J_0(\rho\xi)\right]\frac{\sinh[\xi(H-h)]}{\sinh(\xi H)}\sinh(\xi z)\,\mathrm{d}\xi\\
\mathbf{v}\cdot\mathbf{j} &= B_1U_0a\int_0^{\infty}\frac{xy}{\rho}\xi J_1(\xi\rho)\frac{\sinh[\xi(H-h)]}{\sinh(\xi H)}\sinh(\xi z)\,\mathrm{d}\xi\\
&\quad+B_2U_0a^3\int_0^{\infty}-2\frac{xy}{\rho^2}\xi^2J_2(\xi\rho)\frac{\sinh[\xi(H-h)]}{\sinh(\xi H)}\sinh(\xi z)\,\mathrm{d}\xi\\
\mathbf{v}\cdot\mathbf{k} &= B_1U_0a\int_0^{\infty}-x\xi J_0(\xi\rho)\frac{\sinh[\xi(H-h)]}{\sinh(\xi H)}\cosh(\xi z)\,\mathrm{d}\xi\\
&\quad+B_2U_0a^3\int_0^{\infty}2\frac{x}{\rho}\xi^2J_1(\xi\rho)\frac{\sinh[\xi(H-h)]}{\sinh(\xi H)}\cosh(\xi z)\,\mathrm{d}\xi
\end{aligned}\right\} \tag{23}$$

and

$$q=B_1\mu U_0a\int_0^{\infty}2\frac{x}{\rho}\xi J_1(\xi\rho)\frac{\sinh[\xi(H-h)]}{\sinh(\xi H)}\sinh(\xi z)\,\mathrm{d}\xi. \tag{24}$$

For $h < z < H$ replace $\sinh[\xi(H-h)]$ by $\sinh(\xi h)$, $\sinh(\xi z)$ by $\sinh[\xi(H-z)]$ and $\cosh(\xi z)$ by $-\cosh[\xi(H-z)]$ under the integral sign.

3.2.2. The second step (the correction field)

The correction $\mathbf{w}$ has to satisfy the following boundary condition on the two plates:

$$\mathbf{v}+\mathbf{w}=0. \tag{25}$$

Hence, at $z = 0$,

$$\mathbf{w}\cdot\mathbf{i}=\mathbf{w}\cdot\mathbf{j}=0, \tag{26a}$$

$$\begin{aligned}
\mathbf{w}\cdot\mathbf{k} &= B_1U_0a\int_0^{\infty}x\xi J_0(\xi\rho)\frac{\sinh[\xi(H-h)]}{\sinh(\xi H)}\,\mathrm{d}\xi\\
&\quad-B_2U_0a^3\int_0^{\infty}\frac{2x}{\rho}\xi^2J_1(\xi\rho)\frac{\sinh[\xi(H-h)]}{\sinh(\xi H)}\,\mathrm{d}\xi;
\end{aligned} \tag{26b}$$

and at $z = H$,

$$\mathbf{w}\cdot\mathbf{i} = \mathbf{w}\cdot\mathbf{j} = 0, \tag{27a}$$

$$\mathbf{w}\cdot\mathbf{k} = -B_1 U_0 a \int_0^\infty x\xi J_0(\xi\rho)\frac{\sinh(\xi h)}{\sinh(\xi H)}\,\mathrm{d}\xi + B_2 U_0 a^3 \int_0^\infty \frac{2x}{\rho}\xi^2 J_1(\xi\rho)\frac{\sinh(\xi h)}{\sinh(\xi H)}\,\mathrm{d}\xi. \tag{27b}$$

To solve [1] with the foregoing boundary conditions, the two-dimensional Fourier transform is introduced:

$$\hat{G}(\lambda_1, \lambda_2, z) = \frac{1}{2\pi}\int_{-\infty}^{\infty}\int_{-\infty}^{\infty} g(x, y, z)\exp[i(\lambda_1 x + \lambda_2 y)]\,\mathrm{d}x\,\mathrm{d}y. \tag{28}$$

Note that the caret sign $\hat{}$ denotes a Fourier transform.

The transformed momentum and continuity equations [1] are

$$\left.\begin{aligned} L[\hat{W}_x] &= -\frac{i\lambda_1}{\mu}\hat{S} \\ L[\hat{W}_y] &= -\frac{i\lambda_2}{\mu}\hat{S} \\ L[\hat{W}_z] &= \frac{1}{\mu}\frac{\partial \hat{S}}{\partial z} \end{aligned}\right\} \tag{29}$$

and

$$\frac{\partial \hat{W}_z}{\partial z} - i(\lambda_1 \hat{W}_x + \lambda_2 \hat{W}_y) = 0, \tag{30}$$

where $\hat{S}$ is the pressure associated with the velocity $\hat{\mathbf{W}}$.

The transformed Laplace equation for the pressure is

$$L[\hat{S}] = 0, \tag{31}$$

where

$$L = \frac{\partial^2}{\partial z^2} - \xi^2, \quad \xi^2 = \lambda_1^2 + \lambda_2^2. \tag{32}$$

As proved by Sneddon (1951) it can be shown that the two-dimensional Fourier transform in x and y of $g(x, y, z)$ is equal to the zero-order Hankel transformation if the function to be transformed has the following property: $g(x, y, z) = g(\rho, z)$.

For the transformed boundary condition (see appendix B) we thus get:

at $z = 0$,

$$\left.\begin{aligned} &\hat{\mathbf{W}}\cdot\mathbf{i} = \hat{\mathbf{W}}\cdot\mathbf{j} = 0 \\ &\hat{\mathbf{W}}\cdot\mathbf{k} = -B_1 i U_0 a \frac{\lambda_1}{\xi}\frac{\mathrm{d}}{\mathrm{d}\xi}\left\{\frac{\sinh[\xi(H-h)]}{\sinh(\xi H)}\right\} - B_2 2i U_0 a^3 \lambda_1 \frac{\sinh[\xi(H-h)]}{\sinh(\xi H)}; \end{aligned}\right\} \tag{33a}$$

and at $z = H$,

$$\left.\begin{aligned} &\hat{\mathbf{W}}\cdot\mathbf{i} = \hat{\mathbf{W}}\cdot\mathbf{j} = 0 \\ &\hat{\mathbf{W}}\cdot\mathbf{k} = B_1 i U_0 a \frac{\lambda_1}{\xi}\frac{\mathrm{d}}{\mathrm{d}\xi}\left\{\frac{\sinh(\xi h)}{\sinh(\xi H)}\right\} + B_2 2i U_0 a^3 \lambda_1 \frac{\sinh(\xi h)}{\sinh(\xi H)}. \end{aligned}\right\} \tag{33b}$$

The general solution of [31] can be written as

$$\hat{S} = 2\mu[A\sinh(\xi z) + B\cosh(\xi z)]. \tag{34}$$

The general solution of [29], utilizing [34], can be written as

$$\left.\begin{aligned}\hat{\mathbf{W}}\cdot\mathbf{i} &= C\sinh(\xi z)+D\cosh(\xi z)+\frac{i\lambda_1}{\xi}(H-z)[A\cosh(\xi z)+B\sinh(\xi z)]\\ \hat{\mathbf{W}}\cdot\mathbf{j} &= E\sinh(\xi z)+F\cosh(\xi z)+\frac{i\lambda_2}{\xi}(H-z)[A\cosh(\xi z)+B\sinh(\xi z)]\\ \hat{\mathbf{W}}\cdot\mathbf{k} &= G\sinh(\xi z)+I\cosh(\xi z)+(z-H)[A\sinh(\xi z)+B\cosh(\xi z)].\end{aligned}\right\} \quad [35]$$

Substituting [35] into the transformed continuity equation [30] yields the coupled equation

$$\left.\begin{aligned}A &= i(\lambda_1 C+\lambda_2 E)-\xi I\\ B &= i(\lambda_1 D+\lambda_2 F)-\xi G.\end{aligned}\right\} \quad [36]$$

Introducing [35] into the six transformed boundary conditions [33a, b] the six unknown coefficients, C, D, E, F, G, I may be expressed as functions of A and B. Then, utilizing [36], the following expressions are derived for A and B:

$$A=\frac{\sinh^2(\xi H)}{\sinh^2(\xi H)-\xi^2H^2}\cdot\xi\left[\frac{\xi H}{\sinh(\xi H)}K_2-K_1\right] \quad [37a]$$

and

$$B=\frac{1}{\sinh^2(\xi H)-\xi^2H^2}\cdot\xi\{[\cosh(\xi H)\sinh(\xi H)+\xi H]K_1-[\sinh(\xi H)-\xi H\cosh(\xi H)]K_2\}, \quad [37b]$$

where

$$K_1=\hat{W}_z(z=0);\quad K_2=\hat{W}_z(z=H). \quad [38]$$

Consequently, the explicit expressions for the transformed velocity components of the correction field are

$$\hat{\mathbf{W}}\cdot\mathbf{i}=-\lambda_1^2\frac{F_1(\xi)}{\xi}, \quad [39a]$$

$$\hat{\mathbf{W}}\cdot\mathbf{j}=-\lambda_1\lambda_2\frac{F_1(\xi)}{\xi}, \quad [39b]$$

$$\hat{\mathbf{W}}\cdot\mathbf{k}=i\lambda_1\frac{F_2(\xi)}{\xi} \quad [39c]$$

and

$$\hat{S}=2\mu i\lambda_1\frac{F_3(\xi)}{\xi}, \quad [40]$$

where $F_1(\xi)$, $F_2(\xi)$ and $F_3(\xi)$ are given in appendix D.

In order to obtain $\hat{S}$ and $\hat{\mathbf{W}}$ in the real domain a two-dimensional inverse Fourier transform must be carried out. Since, however, it is identical with the Hankel inverse transform of order zero, the velocity field assumes the form (see appendix C)

$$\left.\begin{aligned}w_x &= -\frac{\mathrm{d}}{\mathrm{d}x}\int_0^\infty\frac{x\xi}{\rho}J_1(\xi\rho)F_1(\xi)\,\mathrm{d}\xi\\ w_y &= -\frac{\mathrm{d}}{\mathrm{d}y}\int_0^\infty\frac{x\xi}{\rho}J_1(\xi\rho)F_1(\xi)\,\mathrm{d}\xi\\ w_z &= -\frac{\mathrm{d}}{\mathrm{d}x}\int_0^\infty J_0(\rho\xi)F_2(\xi)\,\mathrm{d}\xi=\frac{x}{\rho}\int_0^\infty\xi J_1(\rho\xi)F_2(\xi)\,\mathrm{d}\xi,\end{aligned}\right\} \quad [41]$$

and the pressure field is

$$s = 2\mu U_0 a \frac{x}{\rho} \int_0^\infty \xi J_1(\xi\rho) F_3(\xi)\, d\xi. \qquad [42]$$

The complete solution, consisting of reflections up to second order, can be written as

$$\mathbf{u} = \mathbf{v} + \mathbf{w}, \qquad [43]$$

where $\mathbf{v}$ is defined in [23] and $\mathbf{w}$ in [41].

The corresponding pressure field consists of two contributions,

$$p = q + s, \qquad [44]$$

where q is defined in [24] and s in [42].

Higher-order reflection contributions are of order $(a/H)^2$ and are not calculated.

Note that the integrations in [41] and [42] have already been brought into a form ensuring convergence and can be carried out numerically. As an example the pressure distribution along the plates has been calculated. All other integrations can be carried out along the same lines.

3.2.3. The pressure distribution along the plates

A knowledge of the hydrodynamic pressure exerted on the plates is of particular significance in hydrodynamic lubrication, because it sustains the forces exerted on the lubricated element and determines the performance of the journal bearing. A careful check of the expression for the pressure reveals that it consists of two terms, one of which is multiplied by $B_1 U_0 a$, the other by $B_2 U_0 a^3$. The first term is of order a/H, the other term of order $(a/H)^3$. However, reflections of order higher than the second contain terms of order $(a/H)^2$, so that, for second-order reflection solutions, all terms of order higher than (a/H) must be discarded to retain consistency.

After this simplification, a numerical quadrature is carried out along the following lines.

The integrand in [42] is a product of two functions, $F_3(\xi)$ and $J_1(\rho\xi)$, the first of which is positive-definite and tends exponentially to zero, while the second oscillates with a period tending to π for large values of $(\rho\xi)$. Thus, the asymptotic expansion of $J_1(\rho\xi)$ has the form

$$J_1(\rho\xi) = \frac{\sqrt{2}}{\sqrt{\pi\rho\xi}} \cos(\rho\xi - \tfrac{3}{4}\pi). \qquad [45]$$

Equipped with this knowledge, two methods of integration are utilized:

(1) For small values of ρ, integration is carried out between every two consecutive zeros. This results in an alternating, very rapidly converging series, in which every term is larger than the sum of all the following terms. Consequently, an easy criterion of convergence is obtained.
(2) For large values of ξ we used the method, presented by Liron & Mochon (1976).

Thus, if b is real, $F(z)$ is an even function of z, and $F(z)$ decays exponentially along the real axis, the evaluation of a general integral of the following form reads

$$\int_0^\infty J_\nu(bx) x^{\nu+1} F(x)\, dx = \pi i \sum_i \operatorname{res}[F(z) z^{\nu+1} H_\nu^{(1)}(bz)], \qquad [46]$$

where the residues are in the upper half-plane including one-half of the residue at $z = 0$.

With the aid of the above identity, the pressure in its transformed form can be expressed as an infinite series, namely:

$$\frac{p}{\frac{B_1\mu U_0 a}{H^2}} = 12\frac{x}{\rho^2}h\left(1-\frac{h}{H}\right) - 2\pi\frac{x}{\rho}\,\mathrm{Im}\sum_{n=1}^{\infty} H_1^{(1)}\left(\frac{\rho T_n}{H}\right)\left[\frac{T_n^2}{(1+T_n^2)^{1/2}-1}\right.$$

$$\times\left\{\sinh\left(\frac{hT_n}{H}\right)\cosh\left(\frac{T_n}{H}z\right)+\frac{h}{H}\left[\sinh\left(\frac{z-h}{H}T_n\right)+T_n\cosh\left(\frac{z+h}{H}T_n\right)\right.\right.$$

$$\left.\left.-(1+T_n^2)^{1/2}\sinh\left(\frac{z+h}{H}T_n\right)\right]\right\}-T_n\sinh\left(\frac{T_n}{H}z\right)\cosh\left(\frac{T_n}{H}z\right)\Bigg]$$

$$+4\frac{x}{\rho}\sum_{n=1}^{\infty} n\pi\sin\left(\frac{n\pi h}{H}\right)\sin\left(\frac{n\pi}{H}z\right)K_1\left(\frac{n\pi\rho}{H}\right), \qquad [47]$$

where T_n is the root of order n of the equation $\sinh^2 T = T$ in the first quadrant. This representation shows clearly the asymptotic behavior of the pressure with the distance between the plates.

Representation [42] for the pressure converges very rapidly for $\rho > 1$, as can easily be verified.

Figures 3a–c illustrate the pressure variations at the wall $z = 0$ along the lines $y = 0, 0.1\,H, 0.2\,H$, respectively.

3.3. The Drag Force

In this section the drag force exerted on a droplet moving in a quiescent fluid between two stationary plates will be considered. For bubbly lubricating films it is also significant to analyze the case of a free droplet moving in a "Couette" or "Poiseuille" flow.

Based on the reflection solution, the drag force can be calculated by summing up the contribution of each reflection:

$$\mathbf{F}_D = \sum_{i=1}^{\infty} \mathbf{F}_{D_i} \qquad [48]$$

where $\mathbf{F}_{D_i}$ is the drag force due to reflection i.

The generalization of Faxen's law for a spherical fluid particle, as proposed by Hetsroni & Haber (1970), provides a simple technique for obtaining the drag force exerted on the droplet:

$$\mathbf{F}_D = 4\pi\mu a\frac{1+\frac{3}{2}\lambda}{1+\lambda}[\mathbf{v}_\infty - \mathbf{U}]_{\mathbf{r}=\mathbf{0}} + a^3\frac{\lambda}{1+\lambda}[\nabla p_\infty]_{\mathbf{r}=\mathbf{0}}, \qquad [49]$$

where $\mathbf{v}_\infty$ is the unperturbed velocity, $\mathbf{U}$ is the velocity of the droplet, and $\mathbf{r} = \mathbf{0}$ denotes the droplet center.

3.3.1. The drag force of the first reflection

According to the first reflection, the droplet moves in an unbounded stationary field. In this case $\mathbf{v}_\infty = \mathbf{0}$ and $\nabla p_\infty = \mathbf{0}$. Introducing these results into [49] yields

$$\mathbf{F}_{d_1} = -4\pi\mu a\frac{1+\frac{3}{2}\lambda}{1+\lambda}\mathbf{U}\mathbf{i}. \qquad [50]$$

3.3.2. The drag force of an even-number reflection

The second, fourth etc. reflections are regular Stokes solutions between the two plates. Thus, we have

$$\mathbf{F}_{d_{2k}} = 0, \quad k = 1, 2\ldots \qquad [51]$$

3.3.3. The drag force of the third reflection

Equation [49] enables the drag force due to the third reflection to be obtained without an explicit solution of the velocity and pressure fields. The second reflection is considered as the unperturbed velocity field, and the droplet is assumed to be stationary. These velocities are substituted into [49].

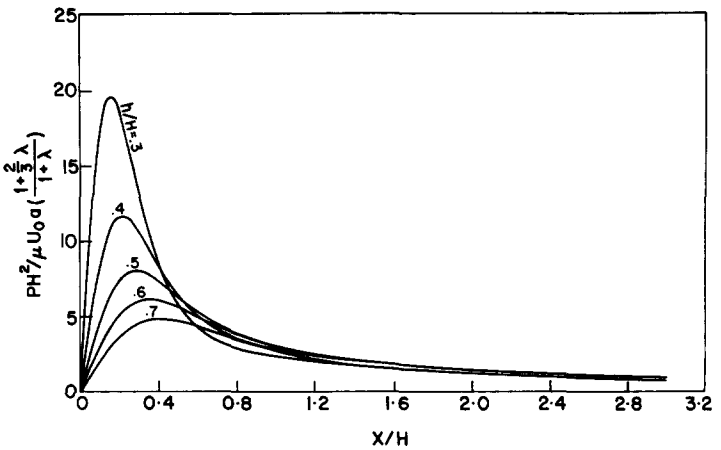

Figure 3a. Variation of wall pressure along a line $y = 0$, $z = 0$.

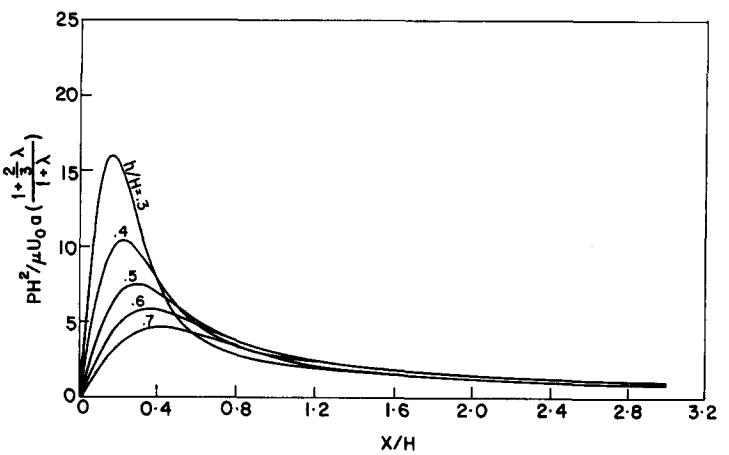

Figure 3b. Variation of wall pressure along a line $y = 0.1\,H$, $z = 0$.

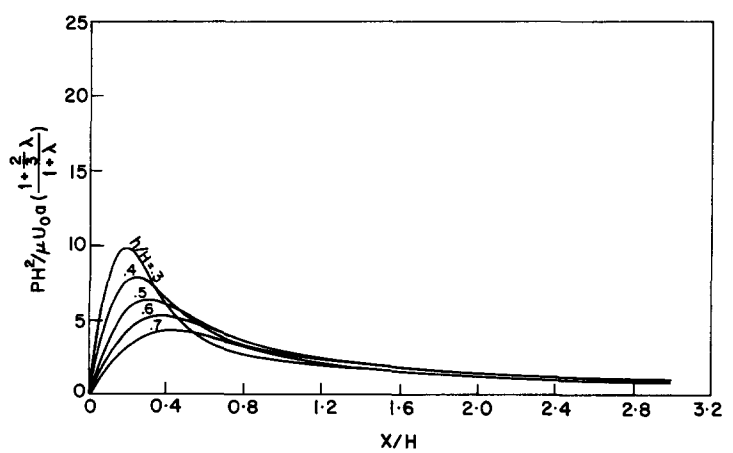

Figure 3c. Variation of wall pressure along a line $y = 0.2\,H$, $z = 0$.

The expression for the drag force in [49] is the sum of two terms—the first is of order a/H, the second of order $(a/H)^3$—as such it must be disregarded in accordance with the approximation order of the solution.

Hence [49] simplifies to

$$\mathbf{F}_{d_2} = 4\pi\mu a \frac{1+\frac{3}{2}\lambda}{1+\lambda}(\mathbf{v} - \mathbf{u}_1 + \mathbf{w})_{r=0}, \quad [52]$$

where $\mathbf{v}$, $\mathbf{u}_1$ and $\mathbf{w}$, are as given in [18], [13] and [41], respectively.

As before, order of magnitude considerations lead to the conclusion that the terms in $\mathbf{v}$ and $\mathbf{w}$ that are preceded by $B_2 U_0 a^3$ must be disregarded.

The expression for $\mathbf{w}$ at the center of the bubble, point $(0, 0, h)$, is (see appendix C)

$$\mathbf{w}(0,0,h) = \left[-\tfrac{1}{2}\int_0^\infty \xi^2 F_1(\xi, z=h)\,d\xi\right]\mathbf{i}. \quad [53]$$

The expression for $(\mathbf{v} - \mathbf{u}_1)$ at the same point is

$$(v_x - u_{x_1})_{r=0} = B_1 \frac{U_0 a}{2}\left[-\frac{1}{2h} + \sum_{n=1}^{\infty}\left(\frac{1}{nH} - \frac{1}{2(h+nH)} - \frac{1}{2(nH-h)}\right)\right], \quad [54]$$

$$(v_y - u_{y_1})_{r=0} = (v_z - u_{z_1})_{r=0} = 0. \quad [55]$$

A different form of [54] is

$$(v_x - u_{x_1}) = B_1 U_0 a\left[-\frac{1}{4h} - \int_0^\infty \exp(-\xi H)\frac{\sinh^2(\xi h)}{\sinh(\xi H)}\,d\xi\right]. \quad [56]$$

Introduction of [50]–[56] into [48] results in an expression for the drag force of order (a/H):

$$F_{D_x} = -4\pi\mu U_0 a \frac{1+\frac{3}{2}\lambda}{1+\lambda}\left(1 + \frac{1+\frac{3}{2}\lambda}{1+\lambda}\frac{a}{H}C_d\right), \quad [57]$$

where

$$C_d = \frac{1}{4}\frac{H}{h} + H\int_0^\infty\left[\exp(-\xi H)\frac{\sinh^2(\xi h)}{\sinh(\xi H)} + \frac{H\xi^2}{B_1 U_0 a}F_1(\xi, z=h)\right]d\xi \quad [58]$$

and $F_1(\xi)$ is given in appendix D, less the term preceeded by $B_2 U_0 a^3$. The drag force factor C_d is described for $h/H = 0.2$ to 0.8 in figure 2. Its numerical values for various locations, h/H, are given in table 1.

Table 1. The drag force factor

h/H	C_d, this solution	C_d, Faxen's solution (Happel & Brenner 1973, p. 326)
0.125	3.0816498	—
0.150	2.6105768	—
0.175	2.2841179	—
0.200	2.0483890	—
0.225	1.8731989	—
0.250	1.7403342	1.7400000
0.275	1.6381566	—
0.300	1.5588909	—
0.325	1.4971622	—
0.350	1.4491596	—
0.375	1.4121359	—
0.400	1.3840958	—
0.425	1.3635972	—
0.450	1.3496225	—
0.475	1.3414952	—
0.500	1.3388281	1.3380000

C_d is symmetric around $h/H = 0.5$.

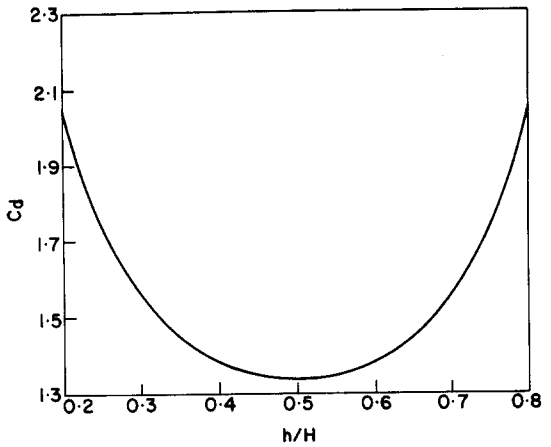

Figure 4. The drag force factor vs droplet location.

Faxen (Happel & Brenner 1973, p. 326) treated the particular case of a *rigid* particle ($\lambda \to \infty$) moving parallel to the plates at $h/H = 1/4$. He utilized a different numerical scheme and obtained $C_d = 1.74$. This is a particular numerical value derived from figure 4 (or table 1) and it validates both schemes of analysis.

3.4. The Equation of the Interface

The analysis presented so far assumes that the droplet is spherical. This is known to be accurately so for a slowly moving droplet in an unbounded quiescent fluid. However, in the presence of the neighboring plates the droplet changes its shape due to the "wall effect". This effect can be analyzed in the manner suggested by Hetsroni & Haber (1970) since, for small deviations from sphericity, the separate contributions of the reflections can be superimposed, and each even-numbered reflection can be regarded as an unbounded unperturbed velocity field embedding a droplet.

For an almost spherical droplet of mean radius a, Hetsroni & Haber (1970) suggested the following representation:

$$r = a[1 + \xi(\theta, \phi)], \qquad [59]$$

where the function describing the deviation from sphericity $\xi(\theta, \phi)$ is made up of the sum of surface harmonics determined via the harmonics of the unperturbed velocity field:

$$\xi(\theta,\phi) = \sum_{n=2}^{\infty} \frac{1}{(n^2+n-2)n(n+1)} \frac{1}{(1+\lambda)\sigma} \times \left\{ \frac{p_n^\infty}{r^n} \frac{n}{2(2n+3)} a^{n+1}[(4n^3+6n^2+2n+3)\lambda + (4n^3+6n^2-4n-6)] + \frac{\phi_n^\infty}{r^n} \cdot \mu n a^{n-1}[(4n^3+6n^2+2n-3)\lambda + (4n^3+6n^2-4n)] \right\}. \qquad [60]\dagger$$

The solid harmonics p_n^∞, ϕ_n^∞, described by Hetsroni & Haber (1970), are defined by Lamb's general representation,

$$\left.\begin{aligned} \mathbf{v}_\infty &= \sum_{n=0}^{\infty} \nabla x(\mathbf{r} x_n^\infty) + \nabla \phi_n^\infty + \frac{n+3}{2\mu(n+1)(2n+3)} r^2 \nabla p_n^\infty - \frac{n}{\mu(n+1)(2n+3)} \mathbf{r} p_n^\infty \\ p_\infty &= \sum_{n=0}^{\infty} p_n^\infty, \end{aligned}\right\} \qquad [61]$$

of the unperturbed velocity and pressure fields.

†A similar expression was derived in Hetsroni & Haber (1970) though the authors hold that [60] is a more convenient representation for $\xi(\theta, \phi)$.

If $\mathbf{v}_\infty$ and p_∞ are not *a priori* described by a spherical coordinate system, ϕ_n^∞ and p_n^∞ can be obtained by a very general method which will now be outlined. With the aid of Euler's theorem for solid harmonics it is easy to demonstrate that, for $n \geqslant 1$,

$$p_n^\infty = \frac{r^n}{n!}\left[\frac{\partial^n}{\partial r^n} p_\infty\right]_{r=0}. \qquad [62]$$

Happel & Brenner (1973, p. 63) have shown that the radial velocity component has the form

$$v_{r_\infty} = \sum_{n=1}^{\infty} \frac{n}{2\mu(2n+3)} r p_n^\infty + \frac{n}{r}\phi_n^\infty. \qquad [63]$$

Thus, for $n = 2$ we obtain

$$\phi_2^\infty = \frac{r^3}{2}\left[\frac{\partial v_{r_\infty}}{\partial r}\right]_{r=0}; \qquad [64a]$$

and for $n \geqslant 3$ the general form of ϕ_n^∞ is

$$\phi_n^\infty = \frac{r^n}{n!}\left\{\left[\frac{\partial^{n-1} v_{r_\infty}}{\partial r^{n-1}}\right]_{r=0} - \frac{(n-1)(n-2)}{2\mu(2n-1)}\left[\frac{\partial^{n-2} p_\infty}{\partial r^{n-2}}\right]_{r=0}\right\}. \qquad [64b]$$

Note that both p_n^∞ and ϕ_n^∞ are solely described by the given functions of $\mathbf{v}_\infty$ and p_∞ and their derivatives.

Introduction of [62] and [64a, b] into [60] demonstrates, in the most general manner, the explicit relation between the deviation from sphericity function $\xi(\theta, \phi)$ and the unperturbed velocity and pressure fields $\mathbf{v}_\infty$ and p_∞.

It can be shown that the nth term in [60] is of order $(a/H)^{n-1}$. Thus, all terms are negligible compared with the first term ($n = 2$). However, since ϕ_2^∞ is of order $(a/H)^4$, the last term must also be disregarded. Consequently, the deviation-from-sphericity function simplifies to

$$\xi(\theta, \phi) = \frac{\mu a}{\sigma}\frac{(19\lambda + 16)}{8(1+\lambda)}\left[\frac{\partial U_{r_\infty}}{\partial r}\right]_{r=0}. \qquad [65]$$

Since a droplet moving in an unbounded stationary field is spherical, the only contribution to the term $[\partial U_r/\partial r]_{r=0}$ that need be considered is the second reflection $\mathbf{u}_2$.

The solution for $\mathbf{u}_2$ is

$$u_2 = \mathbf{v} - \mathbf{u}_1 + \mathbf{w} \qquad [66]$$

where $\mathbf{v}$, $\mathbf{u}_1$ and $\mathbf{w}$ are given in [18], [13] and [41], respectively.

It can easily be shown that the flow field $\mathbf{v} - \mathbf{u}_1$ induced by the image droplets does not contribute to the deformation of the droplet. The contribution of $\mathbf{w}$, however, yields

$$r = a\left[1 + \frac{\mu U_0}{\sigma}\left(\frac{a}{H}\right)^2 \frac{(19\lambda + 16)(3 + 2\lambda)}{48(1+\lambda)^2} \sin\theta \cos\theta \cos\phi \cdot C_s\right], \qquad [67]$$

where

$$C_s = \int_0^\infty \xi^2 [g_2(\xi) - g_1(\xi)]\, d\xi; \qquad [68]$$

$g_1(\xi)$ and $g_2(\xi)$ are given in appendix D.

In figure 5 and table 2, C_s is given for various drop locations $h/H = 0.2$ to 0.8. To illustrate the deviation from sphericity, [67] was evaluated for $h/H = 0.75$. The resulting shape is depicted with a magnified amplitude in figure 6. Under conditions that are physically more plausible the deviation from sphericity will not have such a pronounced amplitude.

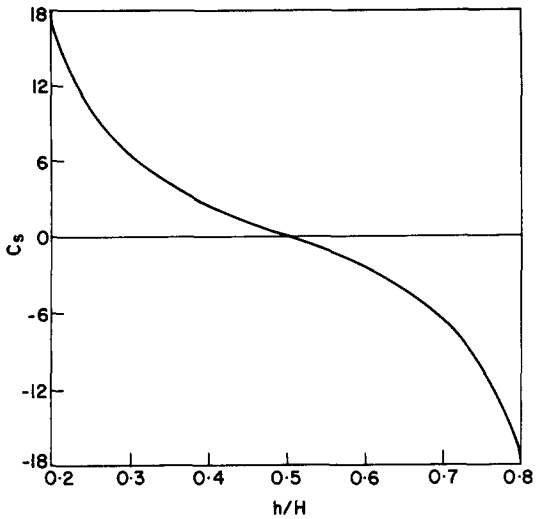

Figure 5. Shape factor vs droplet location.

Table 2. The shape factor

h/H	C_s
1.125	46.855032
0.150	32.064157
0.175	23.113142
0.200	17.277737
0.225	13.254568
0.250	10.355697
0.275	8.1895954
0.300	6.5196094
0.325	5.1953737
0.350	4.1171408
0.375	3.2160993
0.400	2.4429503
0.425	1.7609632
0.450	1.1415566
0.475	0.56133961
0.500	0.00000000

C_s is antisymmetric around $h/H = 0.5$.

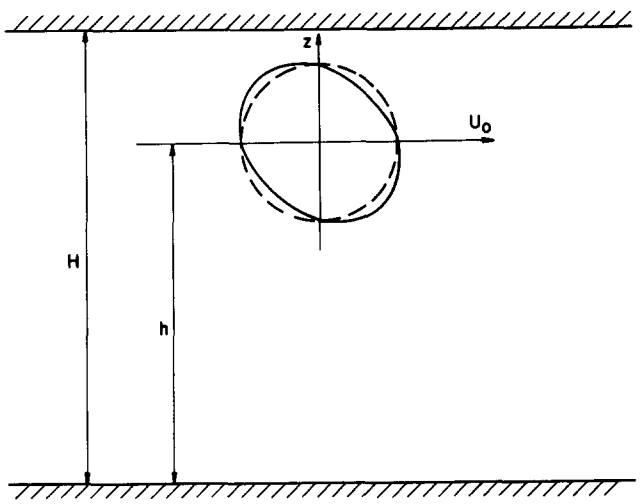

Figure 6. The deviation of the droplet shape from sphericity.

4. DISCUSSION AND CONCLUSIONS

As expected, the pressure distribution, at the parallel plates between which a droplet is located, is antisymmetric and reaches a maximum on the plates at $x_2 = 0$ (plane of symmetry) and $x_1/H = 0.2$ to 0.3. The closer the droplet is to the plates, the higher the pressure peak. The net effect on the plate consists, therefore, of a force parallel to the plane of the plates due to hydrodynamic shear and a couple due to the pressure profile. The latter could be of considerable significance if the oil film of a journal bearing contains a large number of bubbles. The net couple on the journal may alter the geometrical configuration and consequently affect the performance and the stability of the bearing. An exact calculation of the couple by means of the creeping flow solution is, however, impossible. The pressure decay far from the droplet is of order of $1/r$, so that the total moment due to the pressure "tail" becomes infinite. This physically impossible result stems from the invalidity of Stokes' equation at some distance from the droplet. To resolve the difficulty, a Proudman–Pearson solution must be applied.

The wall effect on the drag factor C_d (figure 4) is obviously symmetrical with respect to $h/H = 0.5$ and impedes the motion of the droplet parallel to the plates. The drag increases as the droplet gets closer to the walls, and it assumes a minimum value for $h/H = 0.5$. Theoretically, it increases to

infinity for $h/H = 1$ (or $h/H = 0$). The authors, however, confined the evaluation of the drag factor to the region of droplet locations between $h/H = 0.2$ to 0.8. For regions closer to the walls, the number of reflections used in this work is insufficient to obtain accurate results, due to the slowly converging nature of the reflection solutions at high h/H and a/H ratios.

The wall effect on the shape of a droplet is shown in figure 5. Again, the extent of distortion is greater for droplets close to the walls and vanishes for droplets moving along the center plane. This last result is not strictly correct, but it suffices for the order of approximation used here. Indeed, using higher-order reflections will prove the existence of small deviations from sphericity of the order $(a/H)^3$.

It should be noted that the solutions given for the velocity and pressure fields rely on the assumption that the droplet has a spherical shape. As such it can be viewed as the first interation in the solution procedure. A second iteration must be based on the distorted shape of the droplet. This may give rise to a drag force perpendicular to the plates, as shown in Haber & Hetsroni (1971) for the case of a droplet moving along a circular tube.

Acknowledgement—This work is part of an M.S. Thesis submitted by M. Shapira to the Senate of the Technion, Israel Institute of Technology.

REFERENCES

BRENNER, H. 1961 The slow motion of a sphere through a viscous fluid towards a plane surface. *Chem. Engng Sci.* **16,** 242–251.

COUTANCEAU, M. & THIZON, P. 1981 Wall effect on the bubble behaviour in highly viscous liquids. *J. Fluid Mech.* **107,** 339–373.

DAGAN, Z., PFEFFER, R. & WEINBAUM, S. 1982 Axisymmetric stagnation flow of a spherical particle near a finite planar surface at zero Reynolds number. *J. Fluid Mech.* **122,** 273–294.

DEAN, W. R. & O'NEILL, M. E. 1963 The slow motion of viscous liquid caused by the rotation of a solid sphere. *Mathematica* **10,** 13–27.

GANATOS, P., PFEFFER, R. & WEINBAUM, S. 1978 A numerical solution technique for three-dimensional Stokes flows with application to the motion of strongly interacting spheres in a plane. *J. Fluid Mech.* **84,** 79–111.

GANATOS, P., PFEFFER, R. & WEINBAUM, S. 1980a A strong interaction theory for the creeping motion of a sphere between plane parallel boundaries. Part 1. Perpendicular motion. *J. Fluid Mech.* **99,** 739–753.

GANATOS, P., PFEFFER, R. & WEINBAUM, S. 1980b A strong interaction theory for the creeping motion of a sphere between plane parallel boundaries. Part 2. Parallel motion, *J. Fluid Mech.* **99,** 755–783.

GLUCKMAN, M. J., PFEFFER, R. & WEINBAUM, S. 1971 A new technique for treating multi-particle slow viscous flow: axisymmetric flow past spheres and spheroids. *J. Fluid Mech.* **50,** 705–740.

GOLDMAN, A. J., COX, R. G. & BRENNER, H. 1967a Slow viscous motion of a sphere parallel to a plane wall—I. *Chem. Engng Sci.* **22,** 637–651.

GOLDMAN, A. J., COX, R. G. & BRENNER, H. 1967b Slow viscous motion of a sphere parallel to a plane wall—II. *Chem. Engng Sci.* **22,** 653–660.

GOLDMAN, H. L. & MASON, S. G. 1962 The flow of suspension through tubes. *J. Colloid Sci.* **17,** 448–476.

GOREN, S. L. 1970 The normal force exerted by creeping flow on a small sphere touching a plane. *J. Fluid Mech.* **41,** 619–625.

HABER, S. & HETSRONI, G. 1971 The dynamics of a deformable drop suspended in an unbounded Stokes flow. *J. Fluid Mech.* **49,** 257–278.

HABER, S., HETSRONI, G. & SOLAN, A. 1974 Low Reynolds number motion of two droplets. *Int. J. Multiphase Flow* **1,** 57–71.

HABER, S., SHAPIRA, M. & ETSION, I. 1987 The effect of two-phase lubricant on bearing performance. *ASLE* **30,** 34–40.

HAPPEL, J. & BRENNER, H. 1973 *Low Reynolds Number Hydrodynamics*. Noordhoff, Gronigen.

HETSRONI, G. & HABER, S. 1970 The flow in and around a droplet or bubble submerged in an unbounded arbitrary velocity field. *Rheol. Acta* **9**, 488–496.

HETSRONI, G., HABER, S. & WACHOLDER, E. 1970 The flow-field in and around a droplet moving axially within a tube. *J. Fluid Mech.* **41**, 689–706.

HO, B. P. & LEAL, L. G. 1974 Inertial migration of rigid spheres in two-dimensional unidirectional flows. *J. Fluid Mech.* **65**, 365–400.

HO, B. P. & LEAL, L. G. 1975 The creeping motion of liquid drops through a circular tube of comparable diameter. *J. Fluid Mech.* **71**, 361—383.

LAMB, H. 1932 *Hydrodynamics*. Cambridge Univ. Press, Cambs.

LIRON, N. & MOCHON, S. 1976 Stokes flow for a Stokeslet between two parallel flat plates. *J. Engng Math.* **10**, 287–303.

MIYAMURA, A., IWASAKI, S. & ISHII, T. 1980 Experimental wall correction factors of single solid spheres in triangular and square cylinders and parallel plates. *Int. J. Multiphase Flow* **7**, 41–46.

O'NEILL, M. E. 1964 A slow motion of viscous liquid caused by a slowly moving solid sphere. *Mathematika* **11**, 67–74.

O'NEILL, M. E. 1968 A sphere in contact with a plane wall in a slow linear shear flow. *Chem. Engng Sci.* **23**, 1293–1298.

RALLISON, J. M. & ACRIVOS, A. 1978 A numerical study of the deformation and burst of a viscous drop in an extensional flow. *J. Fluid Mech.* **89**, 191–200.

SANO, O. & HASIMOTO, H. 1978 The effect of two plane walls on the motion of a small sphere in a viscous fluid. *J. Fluid Mech.* **87**, 673–694.

SHAPIRA, M. 1982 The creeping flow field around droplets or bubbles between two parallel flat plates. M.Sc. Thesis, Technion, Israel Institute of Technology, Haifa.

SNEDDON, I. N. 1951 *Fourier Transforms*. McGraw-Hill, New York.

STIMSON, M. & JEFFERY, G. B. 1926 The motion of two spheres in viscous fluid. *Proc. R. Soc.* **111A**, 110–116.

TACHIBANA, M. 1973 On the behavior of a sphere in the laminar tube flow. *Rheol. Acta* **12**, 58–69.

TAYLOR, G. I. 1932 The viscosity of fluid containing small drops of another fluid. *Proc. R. Soc.* **138A**, 41–48.

TAYLOR, G. I. 1934 The formation of emulsion in definable field flow. *Proc R. Soc.* **146A**, 501–523.

WAKIYA, S. 1953 A spherical obstacle in the flow of a viscous fluid through a tube. *J. Phys. Soc. Japan* **8**, 254–257.

YOUNGREN, G. K. & ACRIVOS, A. 1976 On the shape of a gas bubble in a viscous extensional flow. *J. Fluid Mech.* **76**, 433–442.

See Overleaf for Appendices A–D

APPENDIX A

The Lipshitz integral is

$$\frac{1}{(a^2+b^2)^{\frac{1}{2}}} = \int_0^\infty e^{-|a|t} J_0(bt)\,dt, \tag{A.1}$$

$$\sum_{n=-\infty}^{\infty}\left(\frac{1}{r_n}-\frac{1}{R_n}\right)=\left(\frac{1}{r_0}-\frac{1}{R_0}\right)+\sum_{n=1}^{\infty}\left(\frac{1}{r_n}+\frac{1}{r_{-n}}-\frac{1}{R_n}-\frac{1}{R_{-n}}\right). \tag{A.2}$$

Utilizing [A.1], the following expression is obtained for the region $0 < z < H$:

$$S = \sum_{n=1}^{\infty}\left(\frac{1}{r_n}+\frac{1}{r_{-n}}-\frac{1}{R_n}-\frac{1}{R_{-n}}\right)$$

$$= \int_0^\infty \left\{J_0(\xi\rho)[e^{\xi(z-h)}+e^{-\xi(z-h)}-e^{\xi(z+h)}-e^{-\xi(z+h)}]\sum_{n=1}^{\infty} e^{-\lambda 2nH}\right\}d\xi. \tag{A.3}$$

Since

$$\sum_{n=1}^{\infty} e^{-\xi 2nH} = \frac{e^{-\xi H}}{2\sinh(\xi H)} \tag{A.4}$$

we obtain from [A.3],

$$S = -2\int_0^\infty J_0(\xi\rho)\frac{\sinh(\xi h)\sinh(\xi z)}{\sinh(\xi H)} e^{-\xi H}\,d\xi. \tag{A.5}$$

Again utilizing [A.1], the following expressions can be obtained:

for $0 < z < h$,

$$\frac{1}{r_0}-\frac{1}{R_0}=\int_0^\infty [e^{-(h-z)\xi}-e^{-(z+h)\xi}]J_0(\rho\xi)\,d\xi = 2\int_0^\infty J_0(\rho\xi)\sinh(\xi z)e^{-\xi h}\,d\xi; \tag{A.6}$$

and for $h < z < H$,

$$\frac{1}{r_0}-\frac{1}{R_0}=\int_0^\infty [e^{-(z-h)\xi}-e^{-(z+h)\xi}]J_0(\rho\xi)\,d\xi = 2\int_0^\infty J_0(\rho\xi)\sinh(\xi h)e^{-\xi z}\,d\xi. \tag{A.7}$$

Introducing [A.7] and [A.6] into [A.1] we get:

for $0 < z < h$,

$$\sum_{n=-\infty}^{\infty}\left(\frac{1}{r_n}-\frac{1}{R_n}\right)=2\int_0^\infty J_0(\rho\xi)\frac{\sinh[\xi(H-h)]}{\sinh(\xi H)}\sinh(\xi z)\,d\xi; \tag{A.8}$$

and for $h < z < H$,

$$\sum_{n=-\infty}^{\infty}\left(\frac{1}{r_n}-\frac{1}{R_n}\right)=2\int_0^\infty J_0(\rho\xi)\frac{\sinh(\xi h)}{\sinh(\xi H)}\sinh[\xi(H-z)]\,d\xi. \tag{A.9}$$

[See [13] in Liron & Mochon (1976).]

APPENDIX B

In Sneddon (1951) it is shown that the two-dimensional Fourier trnasform is equal to the zero-order Hankel transform if $g(x, y, z) = g(\rho, z)$. Hence,

$$\frac{1}{2\pi}\int\int_{-\infty}^{\infty} F(\rho)\exp[i(\lambda_1 x+\lambda_2 y)]\,dx\,dy = \int_0^\infty \rho J_0(\rho\xi)F(\rho)\,d\rho \tag{B.1}$$

and

$$\frac{1}{2\pi}\int\int_{-\infty}^{\infty} F(\xi)\exp[-i(\lambda_1 x+\lambda_2 y)]\,d\lambda_1\,d\lambda_2=\int_0^{\infty}\xi J_0(\rho\xi)F(\xi)\,d\xi, \tag{B.2}$$

where

$$\rho^2=x^2+y^2;\quad \xi^2=\lambda_1^2+\lambda_2^2.$$

The following case is of interest here:

$$f(x,y)=x\int_0^{\infty}\xi J_0(\rho\xi)g(\xi)\,ds. \tag{B.3}$$

Utilizing [B.1], we can write

$$\frac{f(x,y)}{x}=\frac{1}{2\pi}\int\int_{-\infty}^{\infty} g(\xi)\exp[-i(\lambda_1 x+\lambda_2 y)]\,d\lambda_1\,d\lambda_2. \tag{B.4}$$

Using the inverse Fourier transform we can write

$$g(\xi)=\frac{1}{2\pi}\int\int_{-\infty}^{\infty}\frac{f(x,y)}{x}\exp[i(\lambda_1 x+\lambda_2 y)]\,dx\,dy, \tag{B.5}$$

and differentiating the foregoing [B.5] yields

$$\frac{d}{d\lambda_1}g(\xi)=\frac{1}{2\pi}\int\int_{-\infty}^{\infty} if(x,y)\exp[i(\lambda_1 x+\lambda_2 y)]\,dx\,dy, \tag{B.6}$$

so that

$$f(\lambda_1\lambda_2)=-i\frac{d}{d\lambda_1}g(\xi)=-i\frac{\lambda_1}{\xi}\frac{d}{d\xi}g(\xi). \tag{B.7}$$

The following case is of interest:

$$H(x,y)=\int_0^{\infty}\xi^2\frac{x}{\rho}J_1(\rho\xi)h(\xi)\,d\xi \tag{B.8}$$

and

$$H(x,y)=\int_0^{\infty}-\frac{d}{dx}J_0(\rho\xi)\xi h(\xi)\,d\xi. \tag{B.9}$$

From [B.1] we get

$$\begin{aligned}H(x,y)&=-\frac{d}{dx}\frac{1}{2\pi}\int\int_{-\infty}^{\infty}h(\xi)\exp[-i(\lambda_1 x+\lambda_2 y)]\,d\lambda_1\,d\lambda_2\\&=\frac{1}{2\pi}\int\int_{-\infty}^{\infty} i\lambda_1 h(\xi)\exp[-i(\lambda_1 x+\lambda_2 y)]\,d\lambda_1\,d\lambda_2\end{aligned} \tag{B.10}$$

and

$$H(\lambda_1,\lambda_2)=i\lambda_1 h(\xi). \tag{B.11}$$

APPENDIX C

The inverse Fourier transform of the following cases are of interest.

The first case:

$$\left.\begin{aligned} &\hat{F}(\lambda_1, \lambda_2) = i\lambda_1 f(\xi) \\ &\text{and} \\ &F(x, y) = \iint_{-\infty}^{\infty} F(\lambda_1\lambda_2)\exp[-i(\lambda_1 x + \lambda_2 y)]\,\mathrm{d}\lambda_1\,\mathrm{d}\lambda_2. \end{aligned}\right\} \quad [C.1]$$

Utilizing [B.2] we get

$$F(x, y) = \frac{\mathrm{d}}{\mathrm{d}x}\frac{1}{2\pi}\iint_{-\infty}^{\infty} -f(\xi)\exp[-i(\lambda_1 x + \lambda_2 y)]\,\mathrm{d}\lambda_1\,\mathrm{d}\lambda_2$$

$$= -\frac{\mathrm{d}}{\mathrm{d}x}\int_0^{\infty} \xi f(\xi) J_0(\rho\xi)\,\mathrm{d}\xi. \quad [C.2]$$

Since

$$\frac{\mathrm{d}}{\mathrm{d}x} J_0(\rho\xi) = -\frac{x\xi}{\rho} J_1(\rho\xi), \quad [C.3]$$

we obtain from [C.2]

$$F(x, y) = \frac{x}{\rho}\int_0^{\infty} \xi^2 f(\xi) J_1(\rho\xi)\,\mathrm{d}\xi. \quad [C.4]$$

The second case:

$$\left.\begin{aligned} &\hat{H}(\lambda_1, \lambda_2) = \lambda_1^2 h(\xi) \\ &\text{and} \\ &H(x, y) = \iint_{-\infty}^{\infty} \hat{H}(\lambda_1\lambda_2)\exp[-i(\lambda_1 x + \lambda_2 y)]\,\mathrm{d}\lambda_1\,\mathrm{d}\lambda_2. \end{aligned}\right\} \quad [C.5]$$

Similar analysis to the above, yields

$$H(x, y) = \frac{\mathrm{d}}{\mathrm{d}x}\int_0^{\infty} \frac{x}{\rho}\xi^2 h(\xi) J_1(\rho\xi)\,\mathrm{d}\xi$$

$$= \left(\frac{1}{\rho} - 2\frac{x^2}{\rho^3}\right)\int_0^{\infty} \xi^2 J_1(\rho\xi) h(\xi)\,\mathrm{d}\xi + \left(\frac{x}{\rho}\right)^2 \int_0^{\infty} \xi^3 J_0(\rho\xi) h(\xi)\,\mathrm{d}\xi. \quad [C.6]$$

The third case:

$$\left.\begin{aligned} &\hat{G}(\lambda_1\lambda_2) = \lambda_1\lambda_2 g(\xi) \\ &\text{and} \\ &G(x, y) = \frac{\mathrm{d}}{\mathrm{d}y}\int_0^{\infty} \frac{x}{\rho}\xi^2 g(\xi) J_1(\rho\xi)\,\mathrm{d}\xi \end{aligned}\right\} \quad [C.7]$$

APPENDIX D

$$F_1(\xi)=\frac{1}{\sinh^2(\xi H)-(\xi H)^2}\Bigg[B_1U_0a\Bigg\{z\{h\sinh(\xi H)\cosh[\xi(H-h-z)]$$

$$-H\sinh(\xi h)\cosh(\xi z)\}+\xi Hz\left[H\frac{\sinh(\xi h)}{\sinh(\xi H)}\cosh[\xi(H-z)]-h\cosh[\xi(h-z)]\right]$$

$$+H\sinh(\xi z)\left[\xi Hh\frac{\cosh[\xi(H-h)]}{\sinh(\xi H)}-h\cosh(\xi h)-\xi H^2\frac{\sinh(\xi h)}{\sinh^2(\xi H)}\right.$$

$$\left.+H\sinh(\xi h)\frac{\cosh(\xi H)}{\sinh(\xi H)}\right]\Bigg\}+2B_2U_0a^3\Bigg\{\xi H\sinh(\xi z)\left[\xi H\frac{\sinh[\xi(h-H)]}{\sinh(\xi H)}\right.$$

$$\left.-\sinh(\xi H)\right]-\xi z\{\xi H\sinh[\xi(h-z)]-\sinh(\xi H)\sinh[\xi(H-h-z)]\}\Bigg\}\Bigg], \qquad [D.1]$$

$$F_2(\xi)=\frac{1}{\sinh^2(\xi H)}\Big[B_1U_0a\{h\sinh(\xi H)\cosh[\xi(H-z-h)]-H\sinh(\xi h)\cosh(\xi z)\}$$

$$+2B_2U_0a^3\xi\{\sinh[\xi(H-h)]\sinh[\xi(H-z)]-\sinh(\xi h)\sinh(\xi z)\}\Big]$$

$$+\frac{\xi}{\sinh^2(\xi H)-(\xi H)^2}\Bigg(B_1U_0a\Bigg[\xi Hz\left\{h\sinh[\xi(z-h)]+H\frac{\sinh(\xi h)\sinh[\xi(H-z)]}{\sinh(\xi H)}\right\}$$

$$-\xi hH^2\frac{\sinh(\xi z)\sinh[\xi(H-h)]}{\sinh(\xi H)}-H(H-h)\sinh(\xi h)\sinh(\xi z)$$

$$+z\{h\sinh(\xi H)\sinh[\xi(H-z-h)]+H\sinh(\xi h)\sinh(\xi z)\}\Bigg]$$

$$+2B_2U_0a^3\xi^2\Bigg[z\{\xi H\cosh[\xi(h-z)]+\sinh(\xi H)\cosh[\xi(H-h-z)]\}$$

$$-\frac{\sinh(\xi z)}{\sinh(\xi H)}H\{\xi H\cosh[\xi(h-z)]+\sinh(\xi H)\cosh(\xi H)\}\Bigg]\Bigg), \qquad [D.2]$$

$$F_3(\xi)=\frac{\xi}{\sinh^2(\xi H)-(\xi H)^2}\Bigg(B_1U_0a\Bigg[\xi H\left\{h\sinh\xi(z-h)+H\frac{\sinh(\xi h)}{\sinh(\xi H)}\sinh[\xi(H-z)]\right\}$$

$$+h\sinh(\xi H)\sinh[\xi(H-h-z)]+H\sinh(\xi h)\sinh(\xi z)\Bigg]$$

$$-2B_2U_0a^3\xi\{\xi H\cosh[\xi(h-z)]+\sinh(\xi H)\cosh[\xi(H-h-z)]\}\Bigg), \qquad [D.3]$$

$$g_1(\xi) = \frac{1}{\sinh^2(\xi) - \xi^2}\left[\left[\xi\left\{\frac{\sinh\left(\xi\frac{h}{H}\right)}{\sinh\xi}\left[\cosh\left(\xi\frac{H-h}{H}\right) + \cosh(\xi)\cosh\left(\xi\frac{h}{H}\right)\right]\right.\right.$$

$$\left. - 2\frac{h}{H}\cosh^2\left(\xi\frac{h}{H}\right) - \left(\frac{h}{H}\right)^2\sinh(\xi)\sinh\left(\xi\frac{H-2h}{H}\right)\right\}$$

$$\left. + \left(1 + \frac{\xi^2}{\sinh^2\xi}\right)\left[\frac{h}{H}\sinh(\xi)\cosh\left(\xi\frac{H-2h}{H}\right) - \sinh\left(\xi\frac{h}{H}\right)\cosh\left(\xi\frac{h}{H}\right)\right]\right] \qquad [D.4]$$

and

$$g_2(\xi) = \frac{1}{\sinh^2(\xi)}\left[\frac{h}{H}\sinh(\xi)\cosh\left(\xi\frac{H-2h}{H}\right) - \sinh\left(\xi\frac{h}{H}\right)\cosh\left(\xi\frac{h}{H}\right)\right]$$

$$+ \frac{1}{\sinh^2(\xi) - \xi^2}\xi\left[\left(\frac{h}{H}\right)^2\sinh(\xi)\sinh\left(\xi\frac{H-2h}{H}\right) + \left(\frac{2h-H}{H}\right)\sinh^2\left(\xi\frac{h}{H}\right)\right]. \qquad [D.5]$$